Supplementary Information for

Studying biomineralization pathways in a 3D culture model of breast cancer microcalcifications

Netta Vidavsky[1], Jennie AMR Kunitake[1], Aaron E Chiou[2], Paul A Northrup[3], Teresa Porri[4], Lu Ling[2], Claudia Fischbach[2,5]*, Lara A Estroff[1,5]*

[1]Department of Materials Science and Engineering, Cornell University, Ithaca, NY

[2]Nancy E. and Peter C. Meinig School of Biomedical Engineering, Cornell University, Ithaca, NY

[3]National Synchrotron Light Source II, Brookhaven National Laboratory, Upton, NY

[4]Institute of Biotechnology, Cornell University, Ithaca, NY

[5]Kavli Institute at Cornell for Nanoscale Science, Ithaca, NY

* Corresponding authors

Table 1. Calcium, magnesium and phosphorus concentrations in culture media

Media	**Ca concentration**	**P concentration**	**Mg concentration**
DMEM/F12[1]	1.05 mM	0.95 mM	0.4 mM
Human serum[2,3]	2.25-2.5 mM	0.8-1.45 mM	0.8–0.83 mM
Supplemented DMEM/F12 used in this study	2.2 mM	0.95 mM	0.8 mM

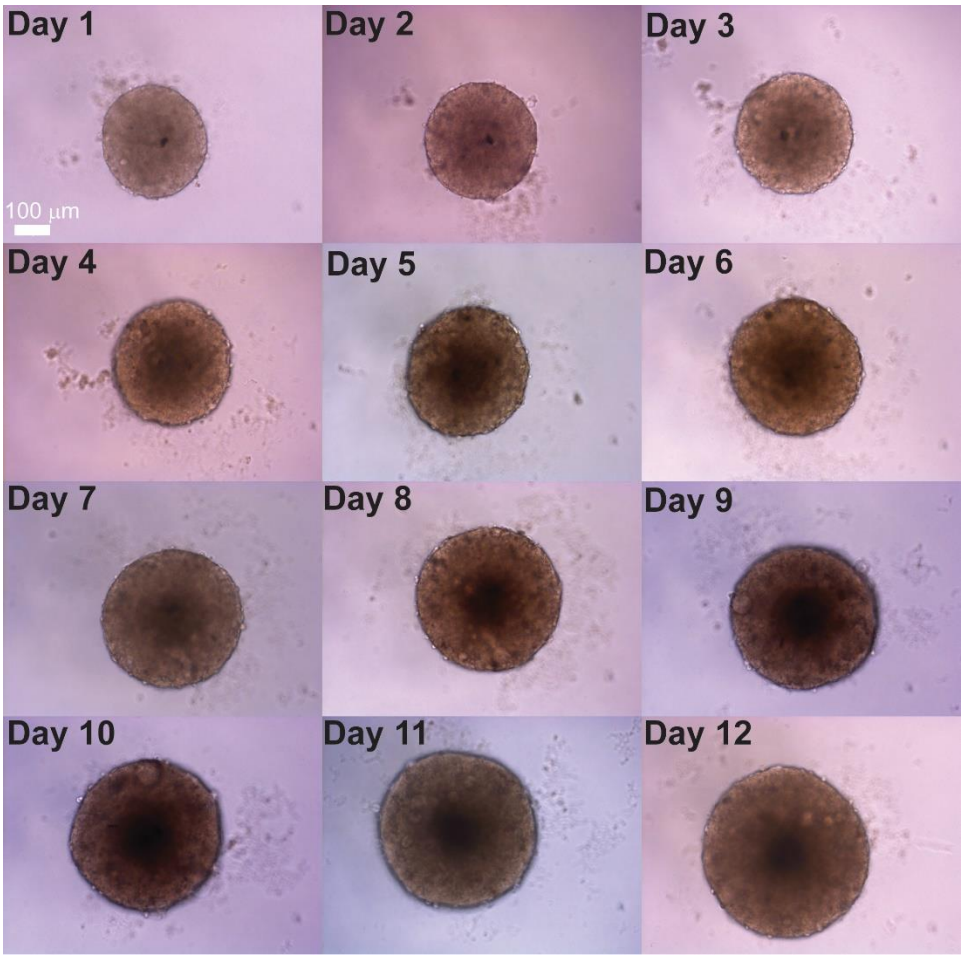

Fig. S1. Light microscope images of MCF10DCIS.com spheroids with time.

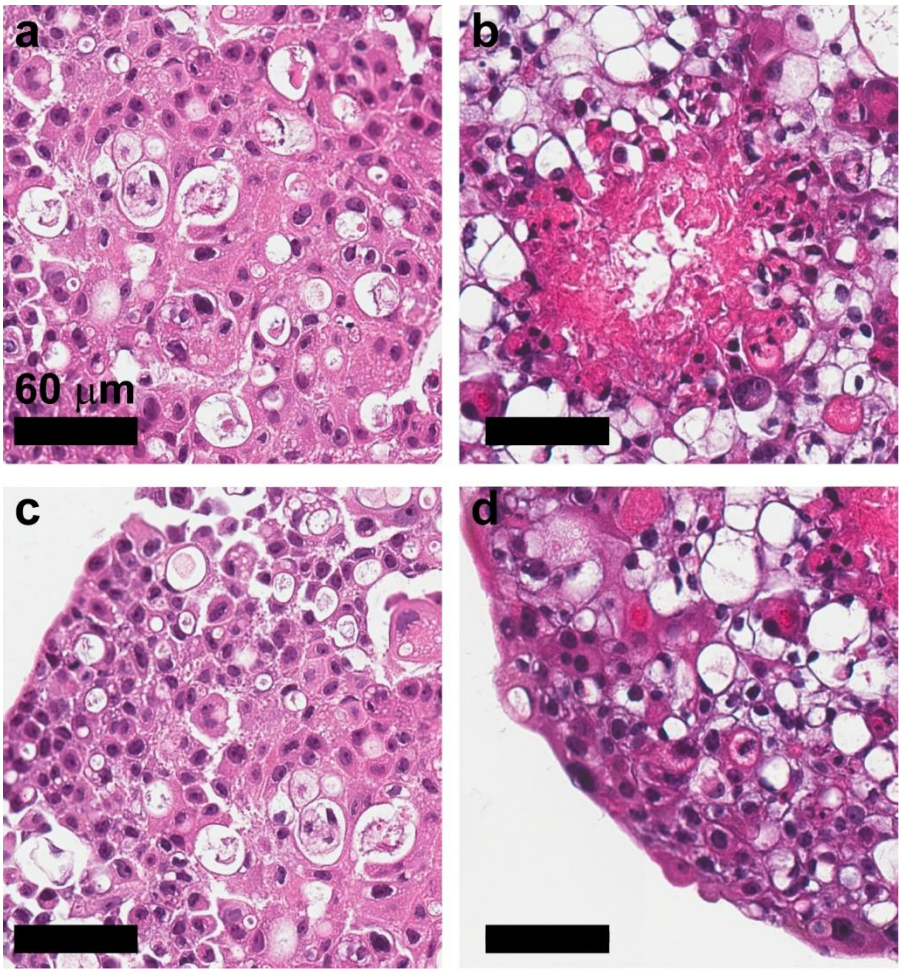

Fig S2. H&E staining (purple: cell nuclei; pink: extracellular matrix, cytoplasm) of paraffin-embedded spheroid cross sections (Day 12). a, c: pre-cancer (MCF10DCIS.com); b, d: invasive (MCF10CA1a). a, b show the spheroid core and c, d show the peripheral viable cell areas. Scale bars: 60 μm.

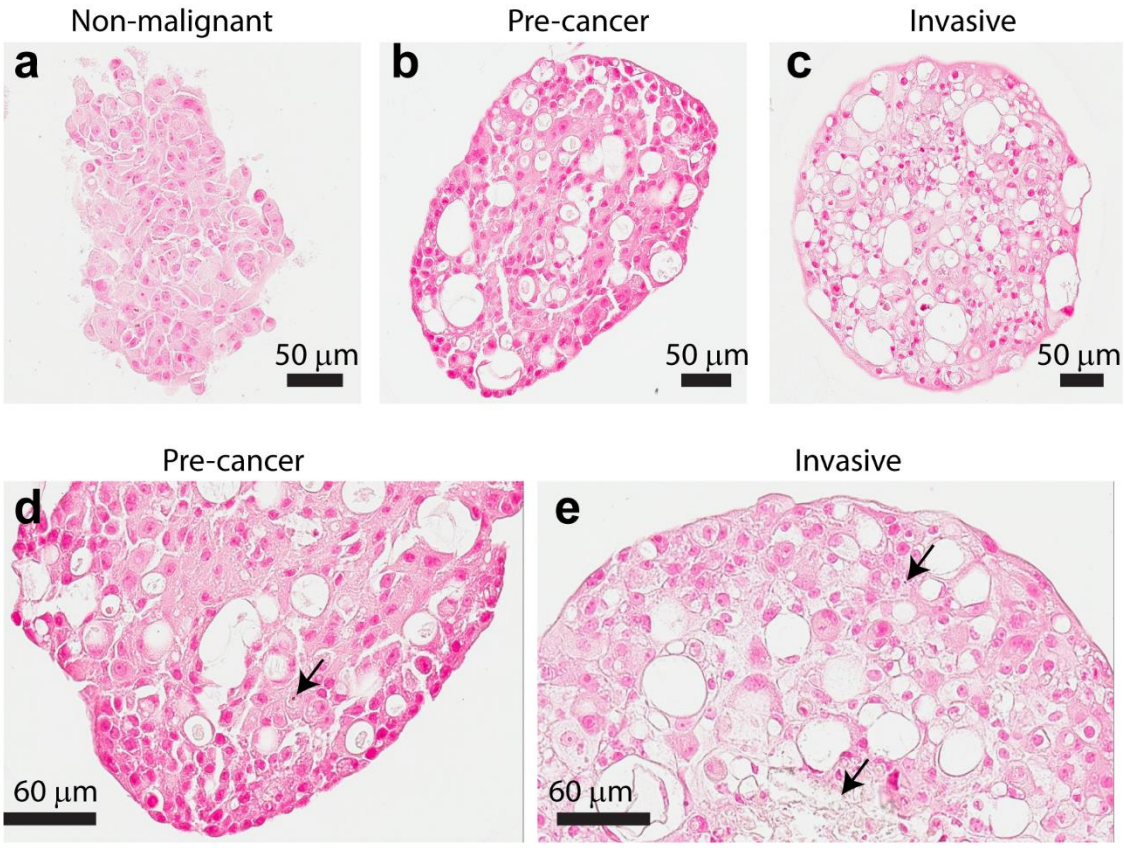

Fig. S3. Von Koss staining (dark brown: phosphate mineral; pink: extracellular matrix) of paraffin-embedded spheroid cross sections (Day 12). a: MCF10A; b, d: MCF10DCIS.com; c, e: MCF10CA1a. The sections in a-c show no mineral staining, while stained particles are shown in d and e (arrows).

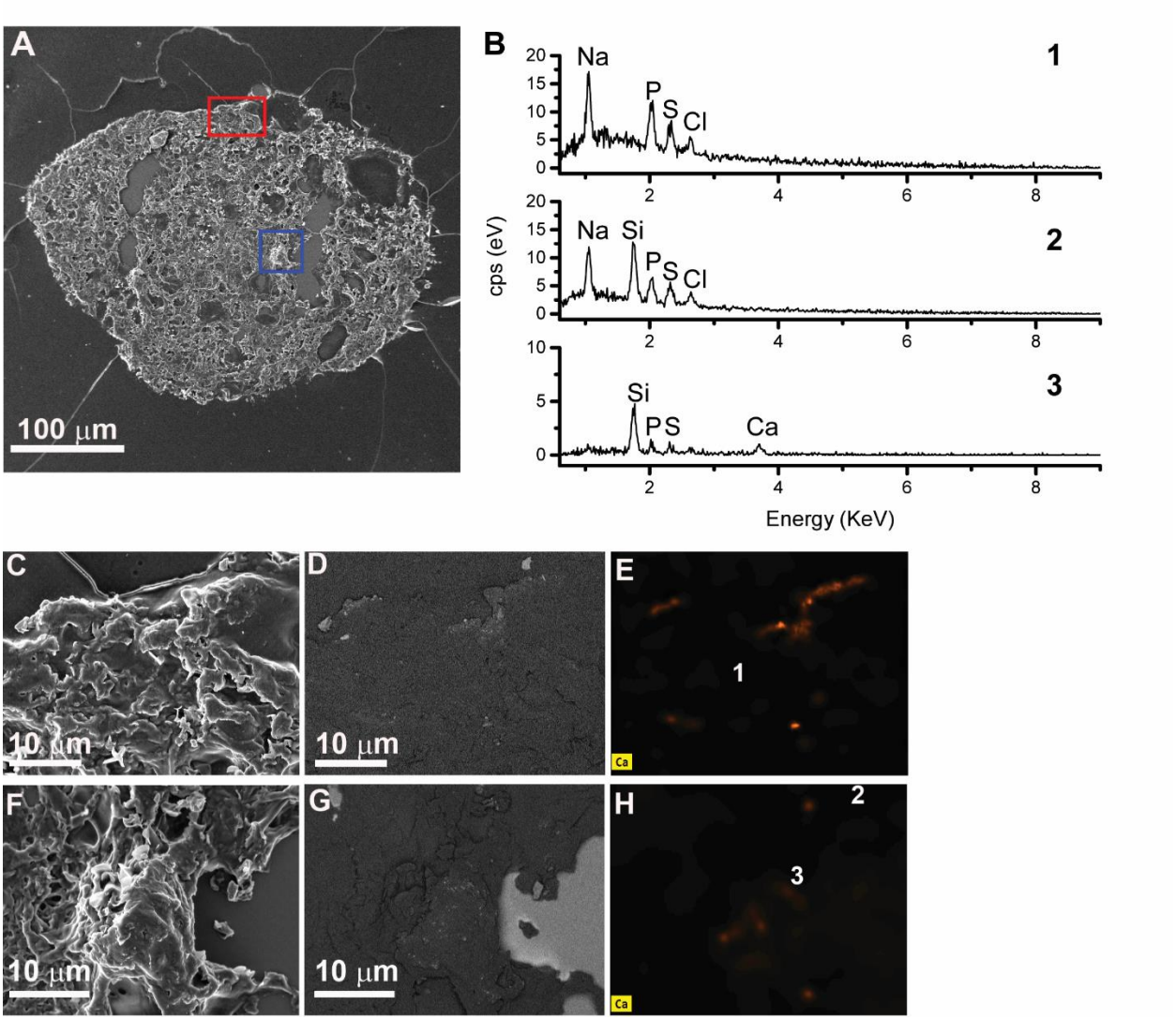

Fig. S4. A: Scanning electron micrograph of secondary electron signal of a spheroid cryo section in which two areas are marked, red-area magnified in C-E and blue-area magnified in F-H. The area marked in blue and shown in F-H is from the same area as in Fig. 2. **B:** EDS spectra obtained from points 1 in E and 2 in H that show no back-scattered electron signal, and 3 in H that does show back-scattered electron signal (and is also shown in Fig. 2). Note that the silicon signal results from the quartz slide substrate. Typical elements to be found in biological tissues such as sodium, sulfur, phosphorus and chlorine are observed. **C, F:** Scanning electron micrograph of secondary electron signal showing a magnification of the areas marked in A, showing the spheroid tissue structure**. D, G:** Scanning electron micrograph of back-scattered electron signal from the same areas as C, F. Bright area to the right is Si substrate. **E, H:** EDS calcium map from the same area as in C-D and F-G. Points 1 and 2 are from areas with no back-scattered electron or calcium signal.

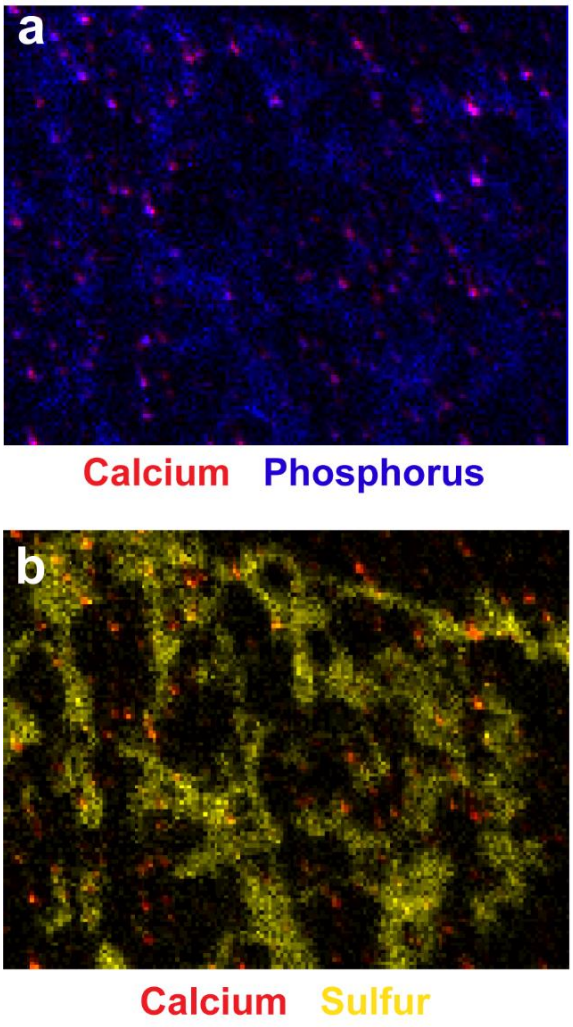

Fig. S5. XRF maps of a DCIS spheroid section (shown in Fig. 2d) showing the overlap of calcium with phosphorus (a) and sulfur (b).

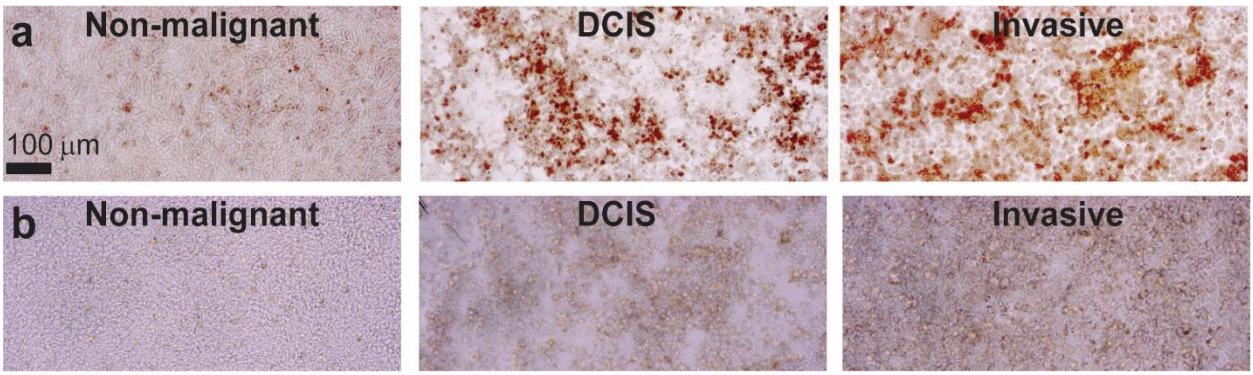

Fig. S6. Mineral formation ability of the MCF10 tumor progression series cells. Alizarin red (**a**) and von Kossa (**b**) staining of MCF10A (non-malignant), MCF10DCIS.com (pre-cancer) and MCF10CA1a (invasive) cells after 10 days of 2D culture.

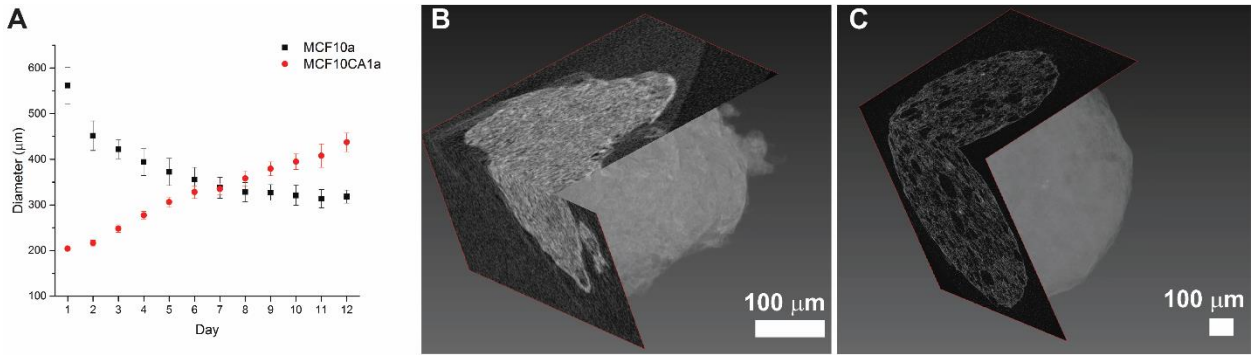

Fig. S7. A: MCF10A and MCF10CA1a spheroid diameter dependence in time, n=10 spheroids with standard deviation as the error bars. Interestingly, the invasive spheroids show a similar linear growth rate to the DCIS, while the non-malignant spheroids actually decrease in size with time. **B, C:** 3D reconstruction of MCF10A (B) and MCF10CA1a (C) spheroids (stained with iodine to increase the contrast of the organic matrix) from nanoCT scan data showing two orthogonal 2D slices of the spheroid and its generated volume.

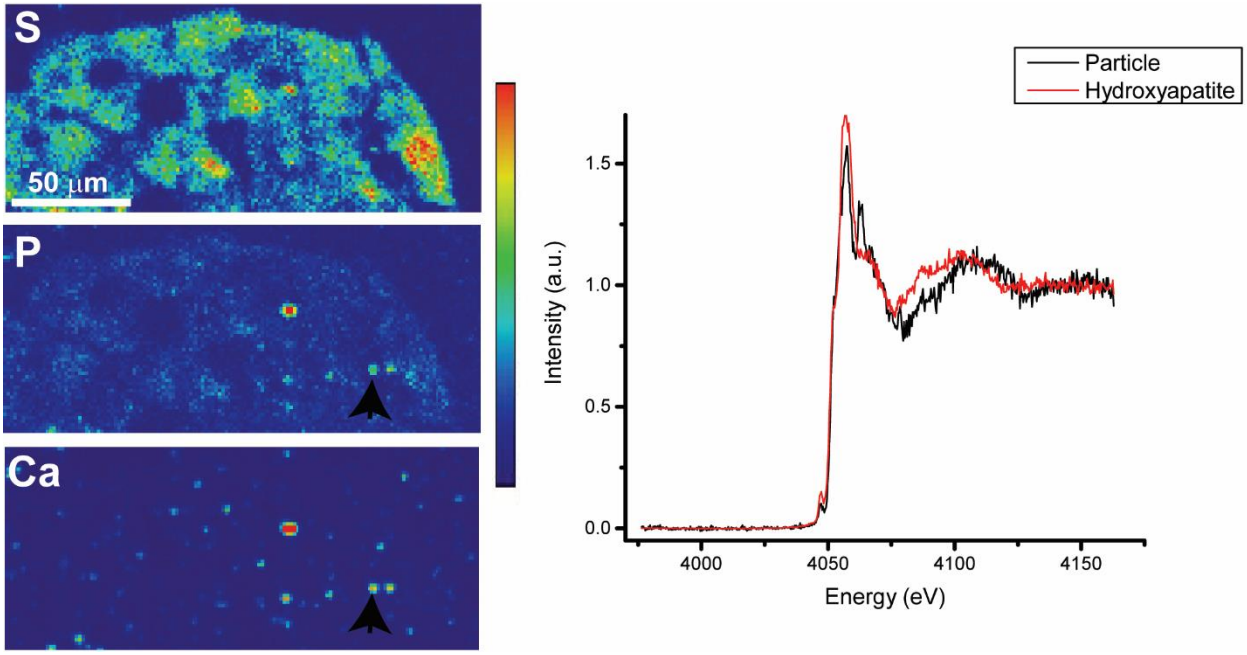

Fig. S8. Mineralized particles in MCF10CA1a spheroids. XRF maps of a spheroid section showing sulfur (S), phosphorus (P) and calcium (Ca) distribution. The sulfur distribution mostly overlaps with the section shape, as sulfur is a typical element found in biological tissues. Phosphorus is also abundant in the section in a dispersed manner, while calcium is more localized in "hot spots". The XANES spectrum of a particle in which strong calcium and phosphorus signals are overlapping (arrows) is shown to the right. Ca K-edge XANES of the marked particle and a hydroxyapatite standard, both measured under the same conditions, are shown. Note that the XANES spectrum shown here is related to the particle with the second highest Ca signal intensity, and not the one with highest intensity that has a noisier spectrum.

Video S9. 3D reconstruction from nanoCT data of an invasive spheroid. The slices forming the spheroid structure are shown in a serial manner, followed by volume rendering to show the spheroid surface. The bright particles observed within the spheroid volume are segmented and labeled in red.

References

(1) Boskey, A. L.; Roy, R. Cell Culture Systems for Studies of Bone and Tooth Mineralization. *Chem. Rev.* **2008**, *108* (11), 4716–4733.

(2) Lundgren, E.; Rastad, J.; Thurfjell, E.; Åkerström, G.; Ljunghall, S. Population-Based Screening for Primary Hyperparathyroidism with Serum Calcium and Parathyroid Hormone Values in Menopausal Women. *Surgery* **1997**, *121* (3), 287–294.

(3) Ma, J.; Folsom, A. R.; Melnick, S. L.; Eckfeldt, J. H.; Sharrett, A. R.; Nabulsi, A. A.; Hutchinson, R. G.; Metcalf, P. A. Associations of Serum and Dietary Magnesium with Cardiovascular Disease, Hypertension, Diabetes, Insulin, and Carotid Arterial Wall Thickness: The ARIC Study. *J. Clin. Epidemiol.* **1995**, *48* (7), 927–940.